Microchimica Acta (2018) 185: 529
https://doi.org/10.1007/s00604-018-3064-3

ORIGINAL PAPER

Graphene nanosheets modified with curcumin-decorated manganese dioxide for ultrasensitive potentiometric sensing of mercury(II), fluoride and cyanide

Alma Mejri[1] · Abdelmoneim Mars[1,2] · Hamza Elfil[2] · Ahmed Hichem Hamzaoui[1]

Received: 26 July 2018 / Accepted: 19 October 2018 / Published online: 6 November 2018

Abstract

A glassy carbon electrode (GCE) was modified by electropolymerization of curcumin on MnO_2-Gr nanosheets to obtain a detection method for Hg(II) and for the anions fluoride and cyanide. The complexation by curcumin can be monitored by potentiometry. The results revealed a cathodic shift for the simultaneous detection of fluoride and cyanide and an anodic shift for the mercury(II) sensing, with peak potentials of −0.24, 0.12 and 0.82 V, respectively (vs. Ag/AgCl). The modified GCE is fairly selective, reproducible and repeatable. The detection limits are 19.2 nM for Hg(II), 17.2 nM for fluoride, and 28.3 nM for cyanide (LOD, S/*N* = 3). The method was successfully applied to the analysis of spiked samples of tap water, river water and petrochemical refinery wastewater.

Keywords Curcumin · Manganese dioxide · Graphene · Mercury(II) · Fluoride · Cyanide · Simultaneous detection · Chronoamperometry · Differential pulse voltammetry

Introduction

The designing of contaminated water sensors has become a dynamic area of research because of the serious chemical problems that affect the ecological system and the human being [1]. Mercury(II), fluoride and cyanide can be considered among the most harmful ones, which accumulate in the environment and subsequently reaches to human [2, 3]. In the same context, the high exposure to these ions affects kidney, respiratory and nervous systems, causing a fatal damage [4]. Furthermore, many major sources of these toxic contaminants can be found citing pesticide production, industrial and medical activities [5, 6]. According to the World Health Organization, the permissible limit of F^-, $CN^-$and Hg^{2+} ion concentrations in drinking water are 1.5, 0.07 and 0.006 μg.mL^{-1}, respectively [7–9].

Varieties of analytical techniques have been employed to quantify trace levels of heavy metals and toxic anions in water citing colorimetric and electrochemical techniques. For instance, N. Ratner et al. have developed sensitive electrochemical gold nanoparticles modified glassy carbon electrode platform for mercury(II) detection. They reported that a remarkable detection limit was found to be 1 μmol.mL^{-1} [10]. Further, P. Borthakur and collaborators have described the use of CoS-reduced porous graphene oxide nanocomposite for the sensing of mercury(II) in aqueous media. The system exhibited a selective response toward Hg^{2+} in the presence of a large variety of interferents with a detection limit of 14.23 nM [11]. Moreover, L. Wan et al. have synthesized a new multifunctional Schiff-based chemosensor, 4,4′-bis(2-hydroxybenzylideneamine)diphenylsulfone (DSS), for simultaneous fluoride and cyanide quantification. The reported work described the use of UV-Vis and photoluminescence spectroscopy (PL) to monitor the detection of target ions [12]. In addition,

Electronic supplementary material The online version of this article (https://doi.org/10.1007/s00604-018-3064-3) contains supplementary material, which is available to authorized users.

✉ Abdelmoneim Mars
abdelmoneim.mars@gmail.com

[1] Valorization Laboratory of Useful Materials (LVMU), National Center of Material Science Research (CNRSM), Techno-park Borj Cedria, BP 273, 8020 Soliman, Tunisia

[2] Laboratory of Natural Water Treatment (LABTEN), Water Researches and Technologies Center, Techno-park Borj Cedria, BP 273, 8020 Soliman, Tunisia

Q. Shu et al. have elaborated a bis(ferrocenyl)phenanthroline iridium(III) complex as a lab-on-a-molecule for the competitive determination of cyanide and fluoride in aqueous solution using the combination of the photoluminescence (PL) and electrochemiluminescence (ECL). The found limit of detection was less than 10 μM in aqueous solution [13]. Moreover, M. Amjadi et al. have described a new chemiluminescence (CL) system based $KMnO_4$-rhodamine B functionalized gold nanoparticles to sense CN^- in real samples such as urine. They reported that the presence of anions inhibited the luminescence response of the system. The linear dynamic range was found to be 0.01–0.50 μM, with a detection limit of 2.8 nM [14].

Curcumin, (E,E)-1,7-bis(4-hydroxy-3-methoxyphenyl)-1,6-heptadiene-3,5-dione, has received much attention due to numerous advantageous properties [15]. K. Ponnuvel et al. have reported the use of a curcumin analog to sense selectively cyanide and fluoride in aqueous media. The fluorescence results revealed a sensitive response toward these two target ions even in the presence of a large range of interferent anions [16]. In the same way, F. Y. Wu and collaborators have described the use of curcumin molecule for monitoring fluoride concentrations in acetonitrile solution. The fluorescence results revealed that the complexation process induces an inhibition of the spectroscopic response of curcumin [17]. Moreover, N. Pourreza et al. have used curcumin nanoparticles to prepare a paper-based analytical device for mercury(II) sensing. The reported work showed that curcumin nanoparticles have an ultrasensitive response toward Hg^{2+} with a linear range of 0.5–20 $\mu g.mL^{-1}$ and a detection limit of 0.17 $\mu g.mL^{-1}$ [18]. Despite all this interest, we did not find until now a work described the use of curcumin in an electrochemical platform for ion detection.

The authors report a new electrochemical mercury(II), fluoride and cyanide platform assay based curcumin modified manganese dioxide-graphene nanosheets. Curcumin is used as both an electrochemical transducer and ion receptor. In addition, the tautomeric forms of curcumin are explored to detect Hg^{2+} as heavy metal cation and F^- and CN^- as toxic anions. Furthermore, the electrochemical studies reveal a potentiometric response with great linear ranges for both target ions. Thus, the chelation process of mercury(II) induces an anodic shift while the recognition of cyanide and fluoride exhibits a cathodic shift. Moreover, the platform exhibits high metrological performances such as the detection limit, repeatability, reproducibility, selectivity and long storage stability. The system is applied to detect target contaminants in various water sources.

Materials and methods

Apparatus and electrodes

Electrochemical measurements were recorded using a MetrohmAutolab PGSTAT 302n electrochemical workstation (Herisau, Switzerland). Experiments were performed at room temperature with a three-electrode system composed of platinum wire as an auxiliary electrode, Ag/AgCl as a reference and the modified glassy carbon electrode as a working electrode. The data were collected using Nova® v1.11 software. SEM images were captured using a MIRA3 LMU Oxford EDX. Raman spectra were recorded using a Horiba LabRam HR Evolution. The XRD pattern was obtained using a Philips X' Pert Pro system.

Reagents and solutions

All reagents were of the highest available grade. Curcumin (CM), graphene oxide, hydrochloric acid (37%), ammonia solution, hydrazine solution (35 wt%), potassium permanganate, $MnSO_4.H_2O$, phosphate buffer tablet, ferricyanide, ferrocyanide, Tertiary-butylammonium salts of anions and mercury(II) chloride were purchased from Sigma-Aldrich (www.sigmaaldrich.com). EIS measurements were carried out using phosphate buffer (PB; 0.1 mM, pH 7.4) containing a mixture of 5 mM of $Fe(CN)_6^{4-}$ and 5 mM of $Fe(CN)_6^{3-}$ was used as a redox probe couple. All experiments have been done at least in triplicate using different platforms.

Preparation of MnO_2-graphene nanosheets

Manganese dioxide-graphene nanosheets were prepared according to reported X. Feng et al. approach [19]. (For more details, see electronic supporting materials).

Preparation of curcumin-MnO_2-graphene nanosheets platform

The curcumin-MnO_2-graphene nanosheets platform was fabricated as described in Fig. 1a. Firstly, the glassy carbon electrode was polished with alumina slurry (a mixture of Υ-Al_2O_3 / water (5 $mg.mL^{-1}$)). The polished surface was sonicated in distilled water. Then, the 5 μL of dispersed MnO_2-Graphene in water (2.0 $mg.mL^{-1}$) was used to coat the GCE surface and it was dried under atmospheric condition. In order to electropolymerized curcumin on the electrode surface, the MnO_2-Graphene-GCE electrode was immersed into the 50 μM curcumin solution in freshly prepared PB (pH 7.4). The 20 consecutive voltammetric cycles were performed in the potential range of [−0.3, 0.6 V] (vs. Ag/AgCl) at the scan rate of 50 $mV.s^{-1}$ [20, 21].

Electrochemical measurement

The DPV measurements were developed using a 5 mL electrochemical cell containing PB (0.1 mM) with a scanning rate of 10 mVs^{-1}. Moreover, the chronoamperometric measurements of the target ion detection were performed at the oxidation potential of the relative curcumin-ion complex.

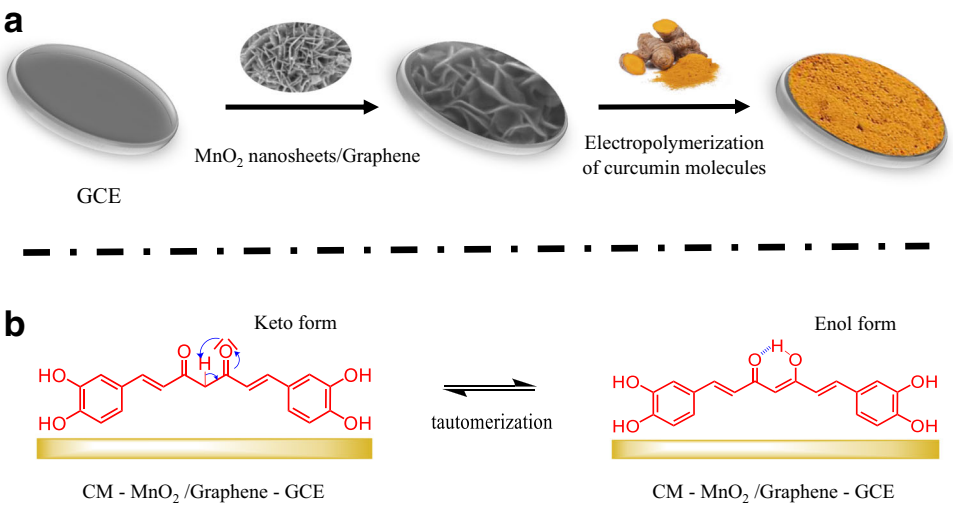

Fig. 1 Schematic representation of the stepwise procedure to prepare Curcumin-MnO_2-Gr platform (**a**) and tautomeric mechanism of the curcumin (**b**)

Additionally, the EIS measurements were performed by applying a 50 mV sinusoidal potential to the working electrode at the frequency range of 0.1 Hz-100 KHz. Furthermore, the determination of fluoride, cyanide and mercury(II) concentrations present in real samples was carried out after a preliminary filtration in order to eliminate the supernatants (for more details, see ESM).

Results and discussion

Choice of materials

Graphene nanomaterials possess unique thermal, mechanical and electrical conductivity properties [22]. This latter has been highly sought to construct sensors and biosensors [23, 24]. Further, manganese oxide nanomaterials as non-toxic metal oxide have been widely in catalysis, energy storage, and sensors [25, 26]. To improve the electron transfer rate and the electrical conductivity of the carbon surface, a combination of these two nanomaterials has been chosen to be integrated into the platform. On the other hand, the choice of the curcumin molecule was fixed because of the dual role of the electrochemical transducer and ion receptor in monitoring the detection event. Indeed, the presence of the two phenolic moieties induces a very stable electrochemical response, even in an aqueous medium. In addition, the α, -diketone group with its two tautomeric forms served as an ion receptor when establishing the detection process (Fig. 1b).

Curcumin-MnO_2-graphene assay design

The curcumin-MnO_2-Gr coated glassy carbon electrode was prepared via the step-by-step strategy. In fact, MnO_2-Gr nanosheets were used to modify GCE due to their electronic proprieties. Further, curcumin with its dual electrochemical transducer-chelator center was used to functionalize the modified electrode surface to explore its tautomeric forms. Indeed, K. Ponnuvel demonstrated that curcumin recognized anions via the enol form while N. Pourreza explained that the keto form ensured the detection of heavy metal cations (Fig. 1b) [16, 18]. Due to this reason, the fabricated curcumin platform was used to detect simultaneously Hg^{2+}, CN^- and F^-. The microscopic, spectroscopic and electrochemical techniques were employed to characterize the Curcumin-MnO_2-Gr platform design.

Microscopic and spectroscopic studies

The MnO_2-graphene nanosheets were integrated into the system design to enhance the electron transfer on the electrode surface. The nanosheet form was elucidated through scanning electron microscopy and atomic force microscopy. In fact, Fig. 2a shows clearly the presence of adsorbed nanosheets on the carbon surface (For the SEM image of CM-MnO_2-Gr, see Fig. S2). In addition, the AFM image reveals the morphology of nanosheets (Inset Fig. 2a). Furthermore, the XRD pattern which was recorded after each preparation steps of MnO_2-graphene, confirms the preparation of the nanosheets. Figure 2b displays the presence of the two diffraction peaks at 22.1° and 42.7° indexed as (002) and (100) respectively relative to graphite. In addition, the diffraction peaks of the nanocomposite indicate the presence of relative MnO_2 diffraction peaks localized at 12.7°, 24.6°, 36.9° and 65.3° relative to (003), (006), (101) and (110) reflections, respectively. To further confirm the formation of MnO_2-graphene nanosheets, Raman spectroscopy was employed. Figure 2c reveals the presence of all characteristic bands relative to the presence of graphene and MnO_2. In fact, Raman spectrum of graphene shows the presence of G band at 1602.1 cm^{-1} relative to the in-plane bond stretching of the pairs of C (sp2) atoms and D band at 1361.3 cm^{-1} relative to breathing modes of rings. As

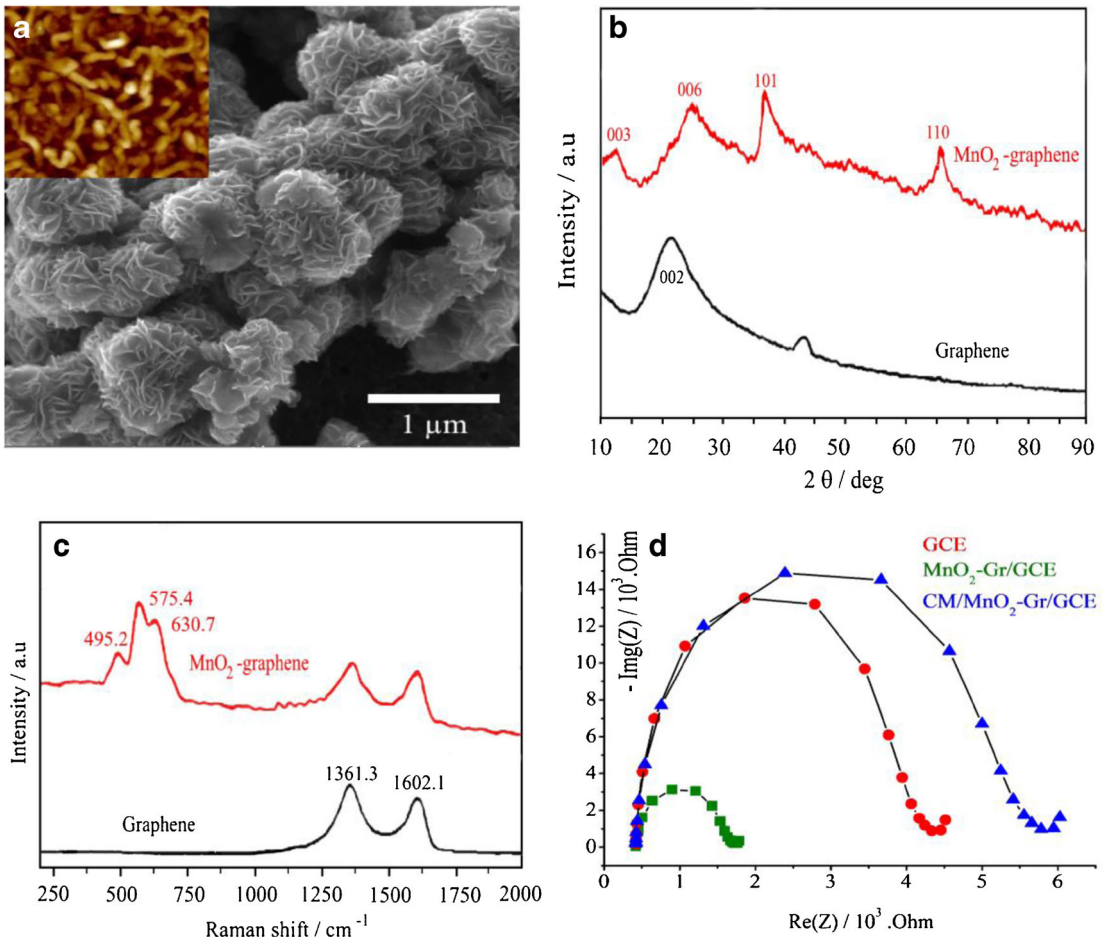

Fig. 2 SEM image of modified MnO_2-graphene nanosheets carbon electrode (inset: AFM image of MnO_2-Graphene nanosheets) (**a**), XRD pattern of MnO_2-graphene nanosheets and graphene nanomaterials (**b**), Raman spectra of MnO_2-graphene nanosheets and graphene nanomaterials (**c**) and Niquist plots of modifications stepwise (**d**)

shown in the Raman spectrum of the nanocomposite, the three major vibration features relative to MnO_2 compound are reported at 495.2, 575.4 and 630.7 cm^{-1}, additionally to characteristic bands of graphene. Moreover, the electrochemical impedance spectroscopy was used to monitor the step-by-step formation of platform design. Figure 2d exhibits the Nyquist plots of the different stepwise of electrode modification. In fact, the coating GCE electrode with MnO_2-graphene nanosheets induced a significant decrease in the charge transfer resistance (R_{ct}) due to its high conductivity compared to the carbon surface. However, the electropolymerization of curcumin exhibited dramatically an enlargement in the semicircle arc leading to a considerable increase in resistance electron transfer.

Electrochemical studies of immobilized curcumin

The immobilization of curcumin (CM) on the modified surface was confirmed by electrochemical techniques such as cyclic voltammetry and differential pulse voltammetry. Indeed, cyclic voltammogram of the modified surface recorded at 50 mVs^{-1} in PB (pH 7.4) reveals the presence of an oxidation peak localized at 0.35 V (vs. Ag/AgCl) and a reduction peak at 0.29 V (vs. Ag/AgCl) relative to the faradic response of curcumin (Fig. S1). Further, Fig. 3a shows the dependence of the logarithm of the oxidation current of CM on the logarithm of the respective scan rates. The plot shows a straight line with a slope near from the unity indicating an adsorption control. Moreover, DPV voltammogram reveals that the oxidation peak current of the immobilized curcumin on the modified electrode is localized at 0.4 V (vs. Ag/AgCl). (Fig. 3b).

Assay of mercury(II), fluoride and cyanide ions

The complexation process which was established between curcumin modified electrode and target ions was monitored using differential pulse voltammetry and chronoamperometry. Due to the presence of two tautomeric forms (enol- keto), the curcumin-based assay platform was able to detect simultaneously cations and anions. In fact, the keto form allowed the cation detection due to the presence of the O,O′-donors

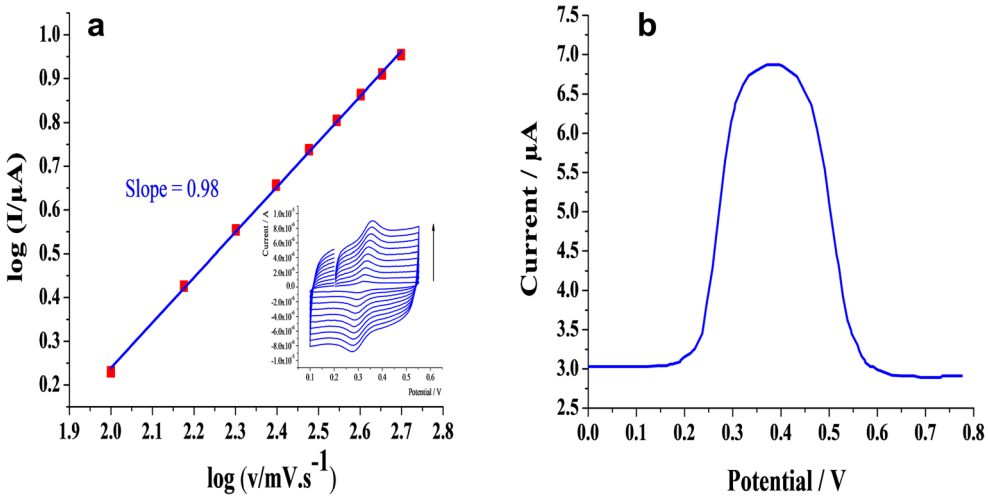

Fig. 3 The plot of the logarithm of the oxidation currents of immobilized CM on modified electrode versus the logarithm of various used scan rates (inset: recorded cyclic voltammograms of modified CM-MnO_2-Gr-GCE electrode at various scan rates) (**a**) and DPV voltammogram of immobilized curcumin on MnO_2-Gr-GCE electrode (**b**)

binding sites. Moreover, the hydroxyl group of enol-form ensured the anion detection via hydrogen bond (Fig. 1b).

Detection of F^- and CN^-

Upon the addition of a small amount of anions into the PB, the DPV results revealed a cathodic potential shift of the oxidation potential, accompanied by a significant decrease in the oxidation current of the free curcumin (Fig. 4a and b). For instance, the addition of 50 ppb of fluoride induced a decrease in the current of the free curcumin by 2.11 μA with a formation of a new DPV peak related to the fluoride-curcumin complex localized at −0.24 V (vs. Ag/AgCl) (Fig. 4b). Besides, the presence of cyanide revealed the appearance of a new oxidation peak at 0.12 V (vs. Ag/AgCl) attributed to the complex formation (Fig. 4a). (For chronoamperograms, see Fig. S3A and Fig. S3B). Furthermore, Fig. 4d shows a linear dependence in the range of *c.a.*50–1200 ppb with a sensitivity of 0.0061 and 0.0052 $\mu A.ppb^{-1}$ for the detection of fluoride and cyanide, respectively. The LOD was found to be 17.2 and 28.3 ppb (LOD, $S/N = 3$) for F^- and CN^-, respectively. Moreover, S. K. Patil et al. interpreted that the cathodic potential shift following the anion detection process is related to the amplification of the electron density of the electrochemical chelator [27].

Detection of mercury(II)

The detection of mercury(II) was also monitored by chronoamperometry and differential pulse voltammetry. The Fig. 4c shows the electrochemical response of the platform toward the presence of Hg^{2+}, which induced an anodic potential shift in contrary to what has been observed in the anion detection. The DPV studies show the appearance of the new oxidation peak of the mercury complex at 0.82 V (vs. Ag/AgCl) (For chronoamperograms, see Fig. S3C). The dependence of the oxidation current of the complex on the concentration of Hg^{2+} reveals a linear response from 50 to 1200 ppb with a sensitivity of 0.00713 $\mu A.ppb^{-1}$ and a LOD of 19.2 ppb (LOD, $S/N = 3$)(Fig. 4d). Beer et al. demonstrated that the anodic shift exhibited by the complexation of cation targets is due to the delocalization of electronic charge from chelator sites towards to a metal center [28]. They explain that the new positively charged cation-receptor complex will be harder to oxidize than the neutral receptor. In addition, it should be emphasized that the simultaneous detection of the three target ions (Hg^{2+}, CN^- and F^-) shows the presence of the oxidation peaks of the corresponding curcumin-target complexes (Fig. S3D).

Analytic performances

To demonstrate the applicability of the curcumin platform, the reproducibility, repeatability, storage stability, selectivity and real test were developed.

Repeatability, reproducibility and storage stability

After measuring the oxidation current exhibited by the complexation of 50 ppb of fluoride for 25 times in a one single day, the relative standard deviation (RSD) of repeatability was calculated to be 3.8%. In addition, RSD of the reproducibility determined by the exploitation of the oxidation current determined by chronoamperometry of six different curcumin platform in the presence of 50 ppb of mercury(II) was calculated. The electrochemical system showed a high reproducibility with 4.2% RSD. Further, three curcumin platforms which demonstrated a high reproducibility were stored at 5 °C for 1 month. The daily electrochemical studies which were recorded by chronoamperometry showed a decrease in the complex peak current by 5.7%. (For chronoelectrochemical results (see electronic supporting materials, Fig. S4 and Fig. S5).

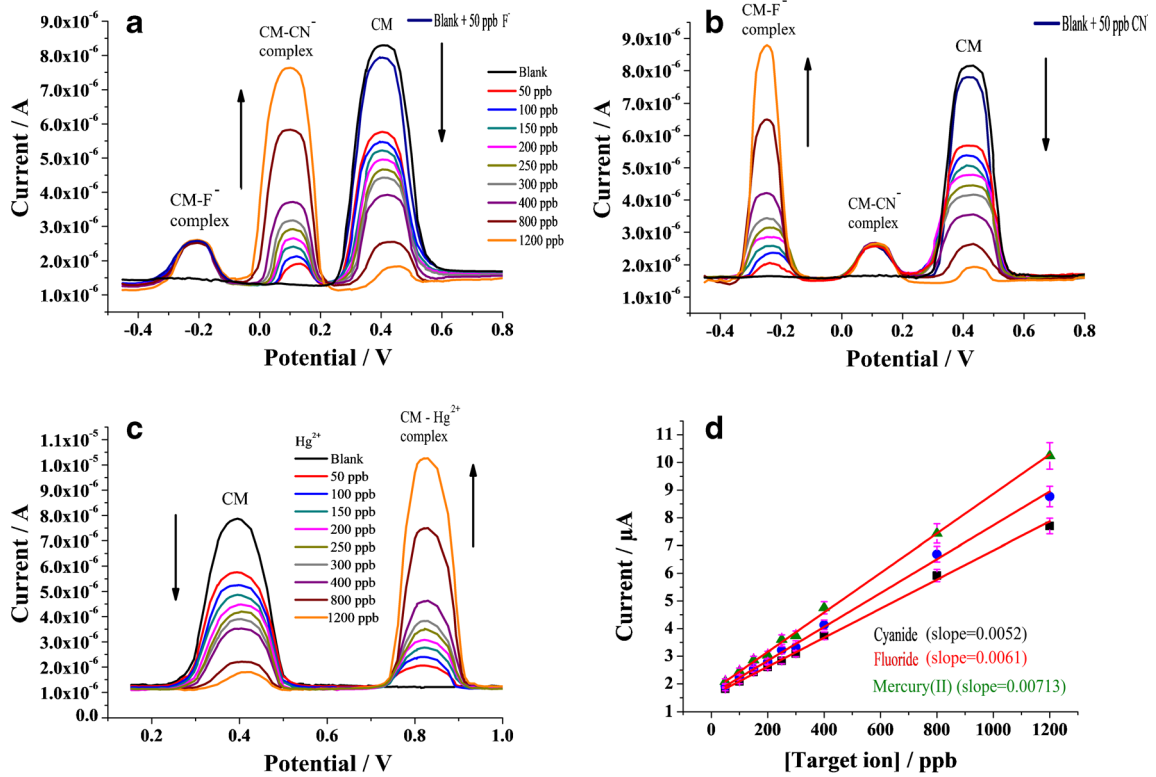

Fig. 4 DPV voltamogrammsof curcumin-MnO_2-Graphene-GCE electrode in the presence of various ion target concentrations from 50 to 1200 ppb recorded at 10 mVs^{-1} scan rate (**a**: cyanide, **b**: fluoride and **c**: mercury(II)) and correlation plots of the assay of target ions (oxidation current of the relative curcumin complex versus the concentration of the target ion) (**d**)

Selectivity and real test

Because of the similarity in the ionic proprieties and to their presence in water, various ranges of ions can be used to demonstrate the selectivity of the curcumin platform toward F^-, CN^- and Hg^{2+}. The electrochemical studies recorded in the presence of a large choice of anions such as I^-, CH_3COO^-, PO_4^{3-}, SCN^- and NO_3^- indicate no considerable decrease in the oxidation peak current of free curcumin, with an absence of a cathodic shift (Fig. 5a). On the other hand, the DPV results recorded in the presence of Mg^{2+}, Fe^{2+}, Zn^{2+} and Cu^{2+}did not shown any remarkable change in the voltammogram of the curcumin platform even in the presence of an amount up to 100 ppm. It is clear from the results that curcumin-based

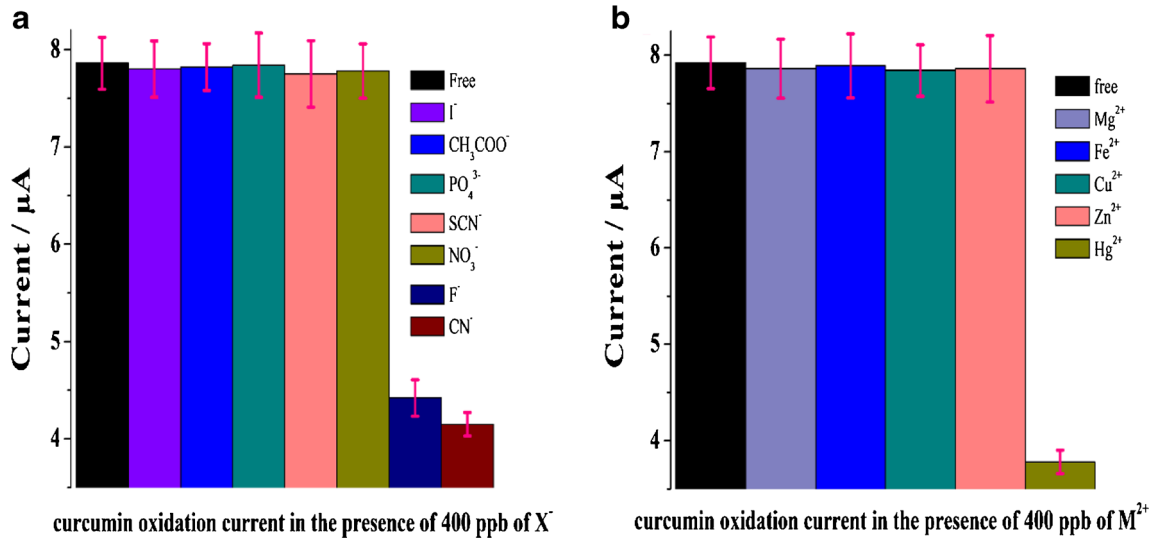

Fig. 5 Histograms of selective results (**a**: anions ions and **b**: cations ions)

Table 1 Determination of target ions in various media

Sample water	Target ion	Detected [Ion] (P) (ppb)	Added [ion] (Q) (ppb)	Detected [ion] after additions (R) (ppb)	Apparent recovery: ((R-P)/Q)*100
Tap water Dilution (10^3)	F^-	232 ± 0.34	100	337.2 ± 0.42	105.2
	CN^-	–	200	202.5 ± 0.37	101.2
	Hg^{2+}	–	200	202.7 ± 0.28	101.3
Medjerda river water Dilution (10^3)	F^-	214 ± 0.31	100	315.4 ± 0.24	101.4
	CN^-	–	400	397.9 ± 0.19	99.47
	Hg^{2+}	–	400	404.3 ± 0.21	101.07
Petrochemical refinery wastewater Dilution (10^3)	F^-	237 ± 0.25	100	341.4 ± 0.22	104.4
	CN^-	127 ± 0.17	200	329.4 ± 0.18	101.2
	Hg^{2+}	164 ± 0.21	200	371.2 ± 0.27	103.6

platform showed a very high selectivity and sensitivity toward target ions even in the presence of numerous interfering ions in aqueous media (Fig. 5b). (For more details, see electronic supporting materials, Fig. S6 and Fig. S7).

To demonstrate its usefulness, the platform was used to detect fluoride, cyanide and mercury(II) in various water samples such as tap and Medjerd a river waters and petrochemical refinery wastewater. It is important to emphasize that a pretreatment step is necessary to remove solid impurities (for more details, see electronic supporting materials). The chronoamperograms, which are summarized in Table 1, reveal a sensitive ability of curcumin MnO_2-Gr platform to detect target ions. (For more electrochemical data, see electronic supporting materials Fig. S8, Fig. S9 and Fig. S10).

Comparative study

To evaluate the curcumin-MnO_2-Gr platform, the found analytic performances were compared with others presented in the literature. It is highly recommended to mention that until now we did not find a reported work that described the use of curcumin as an electrochemical sensor for the detection of both toxic anions and heavy metals. Table 2 reveals that the reported work exhibits a good sensitivity and a low limit of detection compared to those using curcumin as a transducer.

Conclusion

The authors describe the development of new curcumin-based MnO_2-Graphene nanosheets electrochemical platform for the detection of both anions and cations. Fluoride, cyanide and mercury(II) were chosen due to their high toxicity toward human and environmental. Curcumin with its dual enol-keto forms was used as both an electrochemical transducer and ion receptor. The electrochemical results revealed that the detection of F^- and $CN^-$was accompanied by a cathodic shift potential of curcumin oxidation peak, while the detection of mercury(II) was characterized by an anodic shift. Furthermore, the curcumin-based platform revealed very good analytics performances such as the selectivity, reproducibility, repeatability and storage stability. To demonstrate the feasibility of the

Table 2 Summary of works reporting the detection of fluoride, cyanide and mercury(II) ions

Platform	Target ion	Used technique	Sensitivity / LOD	Reference
N, N-dimethyl curcumin	CN^- and F^-	Fluorescence	– / 2.42 nM	[16]
CM NPs based paper	Hg^{2+}	Colorimetric	– / 0.17 ppm	[18]
Curcumin molecule	F^-	Fluorescence	– / –	[17]
Poly(borosiloxane)-based selective electrode	F^-	Potentiometry	–/1 nM	[29]
Au-Nafion-GCE	Hg^{2+}	Potentiometry	11.75 / 3.78 ppb	[30]
Etching of gold nanorods	CN^-	UV-Vis	–/0.5 nM	[31]
CuOnanoshuttles/poly(thionine) modified glassy carbon electrode	Hg^{2+}	Potentiometry	–/8.5 nM	[32]
Gold nanoparticle agglomeration	F^-	Colorimetric	0.5 nM/120 μM	[33]
CM-MnO_2-Gr-GCE	F^-, CN^-, Hg^{2+}	Amperometry	0.006 / 19.2 ppb	Present work

GCE glassycarbonelectrode, *Au* nanogold, *MnO_2* manganesedioxide, *Gr* graphene, *CM* curcumin, *BSA* bovine albuminserum

system, the curcumin-MnO_2-graphene electrode was used to detect target ions in various wastewater and natural waters.

Acknowledgments The authors are grateful to thank the Tunisian Ministry of High Education and Scientific Research for financial support of this work.

Compliance with ethical standards The author(s) declare that they have no competing interests.

References

1. Kruse P (2018) Review on water quality sensors. J Phys D Appl Phys 51:203002
2. Schwarzenbach RP, Egli T, Hofstetter TB, Gunten UV, Wehrli B (2010) Global water pollution and human health. Annu Rev Environ Resour 35:109–136
3. Zulkifli SN, Abdulrahim H, Lau WJ (2018) Detection of contaminants in water supply: a review on state-of-the-art monitoring technologies and their applications. Sensor Actuat B-Chem 255:2657–2689
4. Hanrahan G, Patil DG, Wang J (2004) Electrochemical sensors for environmental monitoring: design, development and applications. J Environ Monit 6:657–664
5. Wang Q, Kim D, Dionysiou D, Sorial G, Timberlake D (2004) Sources and remediation for mercury contamination in aquatic systems – a literature review. Environ Pollut 131:323–336
6. Kjeldsen P (1999) Behaviour of cyanides in soil and groundwater: a review. Water Air Soil Pollut 115:279–308
7. González-Horta C, Ballinas-Casarrubias L, Sánchez-Ramírez B, Ishida MC, Barrera-Hernández A, Gutiérrez-Torres D, Zacarias OL, Saunders RJ, Drobná Z, Mendez MA, García-Vargas G, Loomis D, Stýblo M, Del Razo LM (2015) A concurrent exposure to arsenic and fluoride from drinking water in Chihuahua, Mexico. Int J Environ Res Public Health 12:4587–4601
8. Karmakar A, Kumar N, Samanta P, Desai AV, Ghosh SK (2016) A post-synthetically modified MOF for selective and sensitive aqueous-phase detection of highly toxic cyanide ions. Chem Eur J 22:864–868
9. Frisbie SH, Mitchell EJ, Sarkar B (2015) Urgent need to revaluate the latest World Health Organization guidelines for toxic inorganic substances in drinking water. Environ Health 14:1–15
10. Ratner N, Mandler D (2015) Electrochemical detection of low concentrations of mercury in water using gold nanoparticles. Anal Chem 87:5148–5155
11. Borthakur P, Darabdhara G, Das MR, Boukherroub R, Szunerits S (2017) Solvothermal synthesis of CoS/reduced porous graphene oxidenanocomposite for selective colorimetric detection of Hg(II) ion inaqueous medium. Sens Actuat B-Chem 244:684–692
12. Wan L, Shu Q, Zhu J, Jin S, Li N, Chen X, Chen S (2016) A new multifunctional Schiff-based chemosensor for mask free fluorimetric and colorimetric sensing of F^- and CN. Talanta 152:39–44
13. Shu Q, Birlenbach L, Schmittel M (2012) A bis(ferrocenyl)phenanthroline iridium (III) complex as a Lab-on-a-molecule for cyanide and fluoride in aqueous solution. Inorg Chem 51:13123–13127
14. Amjadi M, Hassanzadeh J, Manzoori JL (2014) Determination of cyanide using a chemiluminescencesystem composed of permanganate, rhodamine B, and gold nanoparticles. Microchim Acta 181: 1851–1856
15. Amalraj A, Pius A, Gopi S, Gopi S (2017) Biological activities of curcuminoids, other biomolecules from turmeric and their derivatives – A review. J Tradit Complement Med 7:205–233
16. Ponnuvel K, Santhiya K, Padmini V (2016) Curcumin based chemosensor for selective detection of fluoride and cyanide anions in aqueous media. Photochem Photobiol Sci 15:1536–1543
17. Wu FY, Sun MZ, Xiang YL, Wu YM, Tong DQ (2010) Curcumin as a colorimetric and fluorescent chemosensor for selective recognition of fluoride ion. J Lumin 130:304–308
18. Pourreza N, Golmohammadi H, Rastegarzadeh S (2016) Highly selective and portable chemosensor for mercury determination in water samples using curcumin nanoparticles in a paper based analytical device. RSC Adv 6:69060–69066
19. Feng X, Zhang Y, Song J, Chen N, Zhou J, Huang Z, Ma Y, Zhang L, Wang L (2014) MnO_2/graphene nanocomposites for nonenzymatic electrochemical detection of hydrogen peroxide. Electroanalysis 26:1–8
20. Mars A, Hamami M, Bechnak L, Patra D, Raouafi N (2018) Curcumin-graphene quantum dots for dual mode sensing platform : electrochemical and fluorescence detection of APOe4, responsible of Alzheimer's disease. Anal Chim Acta, in press 1036:141–146
21. Devadas B, Rajkumar M, Chen SC (2014) Electropolymerization of curcumin on glassy carbon electrode and its electrocatalytic application for the voltammetric determination of epinephrine and p-acetoaminophenol. Colloid Surface B 116:674–680
22. Naumis GG, Barraza-Lopez S, Oliva-Leyva M, Terrones H (2017) Electronic and optical properties of strained graphene and other strained 2D materials: a review. Rep Prog Phys 80:1–63
23. Kuila T, Bose S, Khanra P, Mishra AK, Kim NH, Lee JH (2011) Recent advances in graphene-based biosensors. Biosens Bioelectron 26:4637–4648
24. Shao Y, Wang J, Wu H, Liu J, Aksay IA, Lin Y (2010) Graphene based electrochemical sensors and biosensors: a review. Electroanalysis 22:1027–1036
25. Qui G, Huang H, Dharmarathna S, Benbow E, Stafford L, Suib SL (2011) Hydrothermal synthesis of manganese oxide nanomaterials and their catalytic and electrochemical properties. Chem Mater 23: 3892–3901
26. Zhang J, Jiang J, Zhao XS (2011) Synthesis and capacitive properties of manganese oxide nanosheets dispersed on functionalized graphene sheets. J Phys Chem C 115:6448–6454
27. Patil SK, Ghosh R, Kennedy P, Mobin SM, Das D (2016) Potential anion sensing properties by a redox and substitution series of $[Ru(bpy)_{3-n}(Hdpa)_n]^{2+}$,n=1-3; Hdpa=2,2′-dipyridylamine: selectiverecognition and stoichiometric binding with cyanide and fluoride ions. RSC Adv 6(67):62310–62319
28. Beer PD, Chen Z, Drew MGB, Pilgrim AJ (1994) Electrochemical recognition of group 1 and 2 metal cations by redox-active ionophores. Inorg Chim Acta 225:137–144
29. Puneet P, Vedarajan R, Matsumi N (2016) Alternating poly(borosiloxane) for solid state Ultrasensitivity toward fluoride ions in aqueous media. ACS Sens 1(10):1198–1202
30. Bhanjana G, Dilbaghi N, Bhalla V, Kim K-H, Kumar S (2017) Direct ultrasensitive redox sensing of mercury using a nanogold platform. J Mol Liq 225:598–605
31. Lee S, Nam YS, Choi SH, Lee Y, Lee KB (2016) Highly sensitive photometric determination of cyanide based on selective etching of gold nanorods. Microchim Acta 183:3035–3041
32. Yin Z, Wu J, Yang Z (2010) A sensitive mercury (II) sensor based on CuO nanoshuttles/poly(thionine) modified glassy carbon electrode. Microchim Acta 170:307–312
33. Gu JA, Lin YJ, Chia YM, Lin HY, Huang ST (2013) Colorimetric and bare-eye determination of fluoride using gold nanoparticle agglomeration probes. Microchim Acta 180:801–806